Super-resolution imaging by metamaterial-based compressive spatial-spectral transformation

Qian Ma[1,†], Huan Hu[1,†],Eric Huang[1] and Zhaowei Liu[1,*]
[1]*University of California, San Diego,*
9500 Gilman Drive, La Jolla, California 92093, USA
[†]*These authors contributed equally to this work*
[*]*Corresponding author email address: zhaowei@ucsd.edu*

I. Reconstruction accuracy versus signal noise ratio, sparsity of object and imaging resolution.

The reconstruction accuracy of metamaterial-based compressive spatial-spectral transformation (CSST) is studied numerically under different condition of object sparsity, signal noise ratio and imaging pixel size.

The tuned parameters are

(1) Object Sparsity: number of non-zeros in reconstructed imaging, ranges from 5 to 50 with a step of 2;

(2) Signal Noise Ratio: 10dB to 80dB. Step: 10dB.

(3) Imaging Pixel Size: 6nm and 10nm.

In addition, the total number of object unknowns remains the same (400 pixels).

First, an object is given as randomly switched ON (value 1) pixels on an all zeros 2D matrix. The number of ON pixels equals to the object sparsity. White Gaussian noise (given SNR) is added to the transformed spectrum measurement before reconstruction. Each data point of reconstruction accuracy is then computed through an average of 10 times (each time, both object and noise are randomly generated while SNR and Sparsity are fixed). Second, we increase the pixel size to 10nm from 6nm, which will increase the contrast of encoded spectrums in adjacent pixels. The total number of object unknowns remains the same (400 pixels). Thus, image has relative lower physical resolution (20nm) and larger field of view (200nm × 200nm). It is shown that increasing pixel size will either help reconstruct a less sparse object or improve reconstruction accuracy in a noisier situation. It should also be noted that increasing pixel size will give larger errors in pixelating the object and the illumination patterns. The errors are not discussed here because the pixel size is set to be ~3-4.5 times smaller than smallest feature size of illumination pattern. But the error can no longer be ignored if pixel size gets larger.

II. Dispersion of the object wave

If the scattering response of an object is wavelength dependent, the measurement equations become:

$$I(\lambda) \approx \Delta x \Delta y \sum_{i,j=1}^{N} O(x_i, y_j, \lambda) \cdot H(x_i, y_j, \lambda) \tag{1}$$

A completely unknown $O(x_i, y_j, \lambda)$ cannot be retrieved from above equation. Therefore, other prior-known information is required. Fortunately, in many practical situations, we do know some prior information of the object. We show two working cases here, one simplified case is that the object only consists of one type of particles, and then followed by a more complicated case that the object consists of multiple types of particles. Those cases are very similar to the case of an experimental object tagged by identical scattering particles (such as proteins, or biological organelles, or nano-spheres).

Case #1: The object is made of identical units with an unknown distribution.
In this case, $O(x_i,y_j,\lambda)$ can be simplified into two functions: object distribution function $O'(x_i,y_j)$and response function $S(\lambda)$,

$$I(\lambda) \approx \Delta x \Delta y \sum_{i,j=1}^{N} O'(x_i,y_j) \cdot S(\lambda) \cdot H(x_i,y_j,\lambda) = \Delta x \Delta y \sum_{i,j=1}^{N} O'(x_i,y_j) H'(x_i,y_j,\lambda) \quad (2)$$

where $S(\lambda)$is the intensity response spectrum of a single unit. After independently measuring $S(\lambda)$, one can combined it with $H(x,y,\lambda)$ to generate a modified illumination pattern $H'(x,y,\lambda)$. $O'(x,y)$ can then be retrieved following the same process of non-dispersive case with the modified illumination pattern.

Case #2: The object consists of more than one type of unit (assume q types of units).

$$O(x,y,\lambda) = O'_1(x,y)S_1(\lambda) + O'_2(x,y)S_2(\lambda) + \cdots O'_q(x,y)S_q(\lambda) \quad (3)$$

Thus,

$$(I_\lambda)_{M\times 1} = \begin{pmatrix} H'_1{}_{M\times N^2} & H'_2{}_{M\times N^2} & \cdots & H'_q{}_{M\times N^2} \end{pmatrix}_{M\times (q\cdot N^2)} \begin{pmatrix} O'_1{}_{N^2\times 1} \\ O'_2{}_{N^2\times 1} \\ \vdots \\ O'_q{}_{N^2\times 1} \end{pmatrix}_{q\cdot N^2\times 1} \quad (4)$$

where $H'_1$to $H'_q$are the transfer matrix H modified by S_1 to S_q according to equation [2].
In this case, more unknown variables $(O'_1, O'_2, \dots, O'_q)^T$ are to be solved so that we may suffer from a low reconstruction accuracy. However, Object information O'_1 to O'_q are still retrievable, with a moderate accuracy, by applying other physical constraints to the objects $(O'_1, O'_2, \dots, O'_q)^T$. For example, there should be no overlaps between any two sub-objects O'_i and O'_j.

III. Multilayer Geometry

The multilayer hyperbolic metamaterial consists of alternating Ag and SiO_2 thin layers. It is assumed to be an effective homogenous hyperbolic metamaterial. The HMM is covered by a 40nm thick Cr film, with 20 cylindrical nanoholes. All nanoholes are identical. The hole diameter is 10nm and the hole depth is 40nm.

IV. Transformation Matrix.

The transformation matrix is calculated from the illumination profile of a single nanohole and a known distribution of multiple identical nanoholes. The image area is pixelated to 20 × 20 pixels. For each wavelength channel, the structured illumination pattern is calculated as a linear superposition of illumination profile from all nanoholes. The matrix has size of 200 × 400 (for one polarization) and 400 × 400 (for two polarizations). Wavelength is measured through 400nm to 1200nm, with 4nm per step.

V. Number of Nanoholes

Approximately, every nanohole represents a "1D" sampling of a 2D object from a given projection angle. If there were enough nanoholes to sample an object from every projection angle, the transformation from object to spectrum through CSSTM is then close to a discrete Radon transformation (like a computational tomography). In this exemplary compressive sensing case, only 20 random holes (therefore, 20 project angles for our 20 x 20 pixels image) are selected in our demonstration.
In principle, adding more nanoholes potentially increases the number of projection angles leading to more independent measurements and a larger imaging size. However, the number of measurements of CSSTM

are actually limited by its total number of wavelength channels (400 measuring points for 2 polarization) in that case.

VI. Multiple Nanohole Distribution

The rule of nanohole distribution is that no two positions within the area of interest have the same wavelength coding. This could be mathematically analyzed by the mutual coherence [reference 35 from the manuscript] of the sensing matrix made by all the illumination patterns.

Given an imaging area of interest 120nm×120nm (or 200nm×200nm), nanoholes are randomly placed on the bottom side of the hyperbolic multilayer within a given area 1.7μm×1.7μm. The distance between any two holes should be larger than the illumination pattern resolution: 27nm. For a given distribution, one can calculate the its sensing matrix. The code selects a sensing matrix that has minimum mutual coherence from 10^4 random distributions those nanoholes.

VII. Software

We use COMOSL 4.1a to perform full wave simulation of hyperbolic metamaterial and Matlab 2014b to perform imaging reconstruction via sparse based algorithms. The sparse based algorithm used in this work is l1-ls[26].

Supplementary Figures

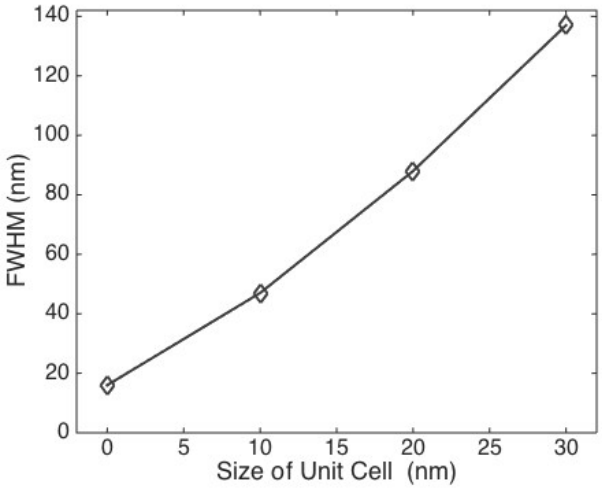

Figure S1. Beam width at HMM and air interface versus unit cell size of HMM. HMM consists of alternating layers of Ag and SiO_2. The filling ratio: 0.5. Total thickness of HMM: 120 nm. Unit Cell Size: 0 nm (effective media theory), 10 nm, 20 nm and 30 nm.

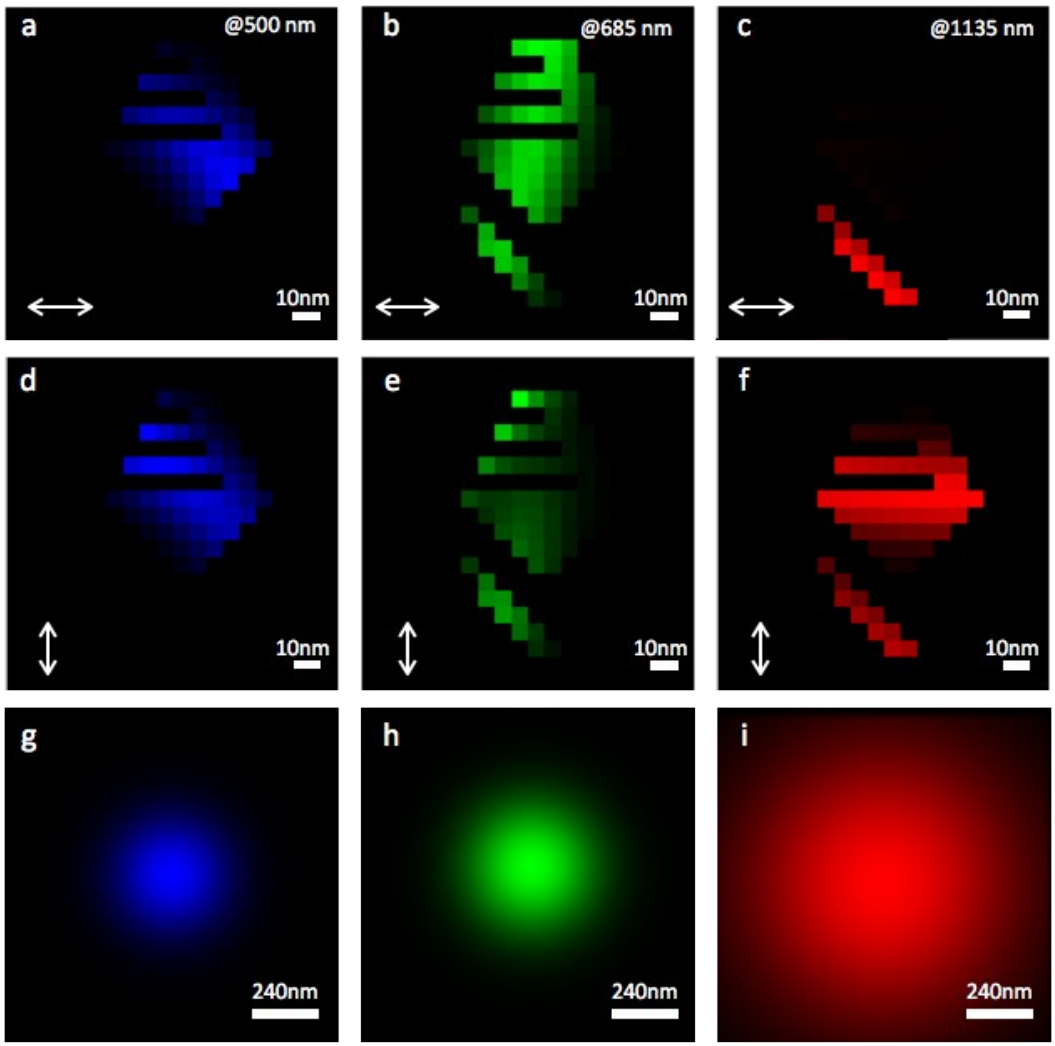

Figure S2. Object illuminated by different wavelengths and two polarizations. (a) Wavelength: 500nm, polarization: 0 degree. (b) Wavelength: 685nm, polarization: 0 degree. (c) Wavelength: 1135nm, polarization: 0 degree. (d) Wavelength: 500nm, polarization: 90 degree. (e) Wavelength: 685nm, polarization: 90 degree. (f) Wavelength: 1135nm, polarization: 90 degree. (g-i) Diffraction-limited image of illuminated objects under 500nm, 685nm and 1153nm, respectively (0^o polarization)

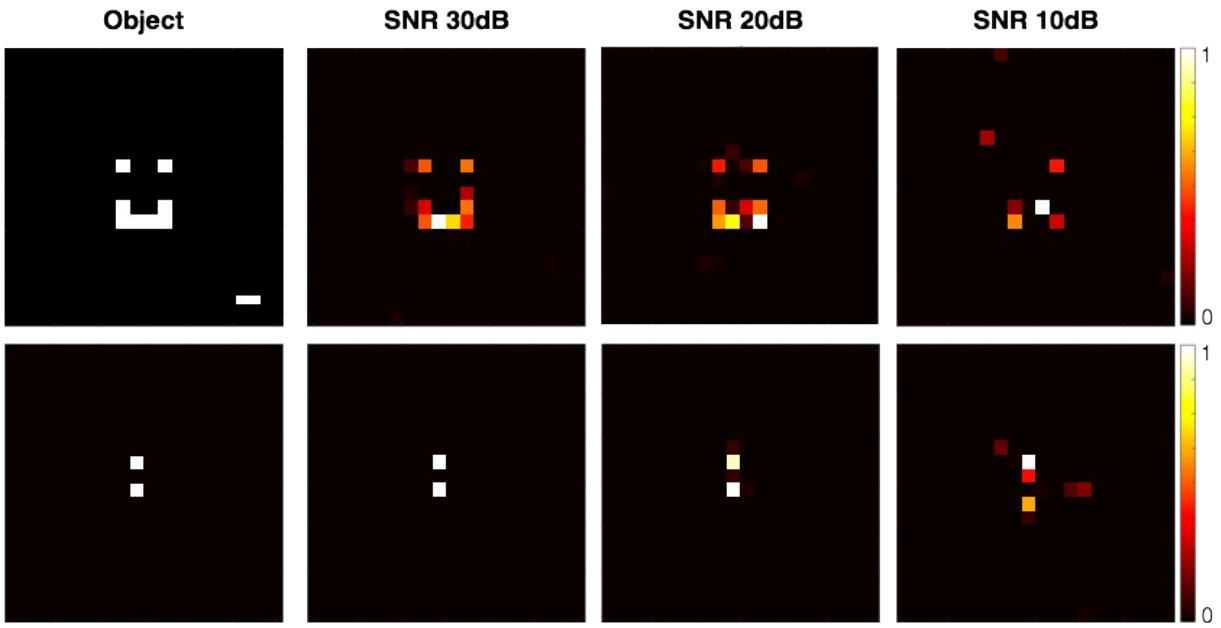

Figure S3. CSST reconstruction results with various noise conditions. Two objects have different sparsity conditions: The first row 'Smile Face' object and second row 'Two Dots' have 8 and 2 non-zero pixels (out of 400 total pixels), respectively. White Gaussian noise is added to the computed spectrum before reconstruction. Column 2 to 4 show reconstructed images of these two objects under different signal noise ratio [30dB, 20dB, 10dB]. Scale Bar: 10nm